ACS APPLIED POLYMER MATERIALS

Article

Cite This: ACS Appl. Polym. Mater. 2020, 2, 791−804

pubs.acs.org/acsapm

Photoresponsive Azobenzene Materials Based on Pyridine-Functionalized Benzoxazines as Surface Relief Gratings

Ahmed F. M. EL-Mahdy,[†,‡] Fang-Wen Lin,[†] Wei-Hung Su,[†] Tao Chen,*[,§] and Shiao-Wei Kuo*[,†,∥]

[†]Department of Materials and Optoelectronic Science, Center of Crystal Research, National Sun Yat-Sen University, Kaohsiung 80424, Taiwan

[‡]Chemistry Department, Faculty of Science, Assiut University, Assiut 71516, Egypt

[§]Ningbo Institute of Material Technology and Engineering, Chinese Academy of Science, Zhongguan West Road 1219, 315201 Ningbo, China

[∥]Department of Medicinal and Applied Chemistry, Kaohsiung Medical University, Kaohsiung 807, Taiwan

Supporting Information

ABSTRACT: We describe the one-pot syntheses of an azobenzene- and pyridine-functionalized benzoxazine monomer (PAPBZ) and a main chain-type polybenzoxazine (BAPBZ) through Mannich condensations of a diamino- and azobenzene-containing pyridine derivative (azo-pyridine-2NH_2), paraformaldehyde, and either phenol or bisphenol in a mixture of toluene and EtOH. Fourier transform infrared (FTIR) and nuclear magnetic resonance (NMR) spectroscopy confirmed the chemical structures of the benzoxazine monomer and polymer. The thermal curing behavior and stability of these benzoxazines were monitored using differential scanning calorimetry, FTIR spectroscopy, and thermogravimetric analysis; the PAPBZ monomer underwent complete ring-opening polymerization to form its polybenzoxazine, while the BAPBZ polymer also underwent thermal curing to give a high-density cross-linked polybenzoxazine. Because of the photoresponsive azobenzene units in the benzoxazine monomer and in the main chain of the polybenzoxazine, these materials exhibited photoresponsivity through reversible photoinduced trans-to-cis isomerization under UV irradiation. The degrees of isomerization of PAPBZ and BAPBZ were 19.3 and 13.9%, respectively. In addition, we used these materials to fabricate surface relief gratings exhibiting interference patterns with tunable long-range order. Accordingly, such azobenzene- and pyridine-functionalized benzoxazines appear to have applicability within optical devices and optical storage media.

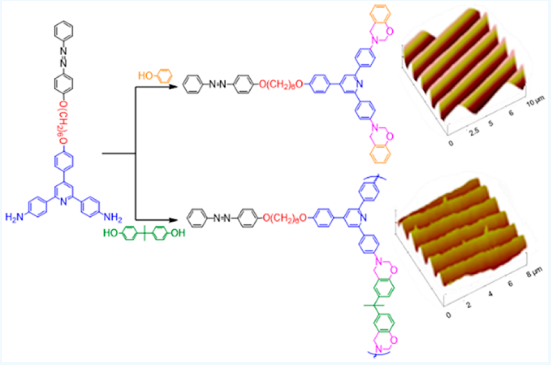

KEYWORDS: *azobenzene, pyridine, benzoxazine, trans-to-cis, surface relief gratings*

INTRODUCTION

Because of their ability to undergo trans-to-cis photoisomerization, azobenzene chromophores have been used widely as building blocks in various stimuli (photo)-responsive supramolecular compounds.[1−4] Hartley et al. discovered the photoisomerization of the azo chromophore, which experiences photoinduced trans-to-cis isomerization under irradiation with a UV lamp and cis-to-trans isomerization upon being left in the dark or heating.[1] The photoresponsive nature of azobenzene chromophores can result in remarkable changes in visual color, dipole moment, and molecular orientation.[5] Significant examples of the use of azobenzene compounds in photochemical switching applications include light-triggered nanocarriers, photoactuators, host/guest systems, species displaying photocontrolled supramolecular chirality, micropatterning, photoregulated liquid crystal polymers, and optically switchable electronic devices.[6−18] Furthermore, azo-containing supramolecular polymeric materials have also been synthesized and considered as suitable candidates for polarization holography and data storage.[19−27] Unfortunately, because of typically low glass transition temperatures, azo-containing compounds and polymers have tended to exhibit poor thermal stability, which has restricted their applicability in photoresponsive systems.[28] Therefore, the challenge remains to design azo-containing polymers displaying high degrees of thermal stability. Recently, we reported the preparation of a thymine- and azo-functionalized conjugated polymer (PTCAz-T) through a combination of a click reaction and Suzuki coupling polymerization. The resultant polymer exhibited a high degree of thermal stability due to a large number of strong T···T hydrogen bonds that restricted its molecular motion and constricted its free volume.[29] In addition, we also reported a supramolecular complex PVB-DAP/azo-T featuring hydrogen bonding between the polymer PVB-DAP and the thymine-

Received: November 13, 2019
Accepted: December 12, 2019
Published: December 12, 2019

DOI: 10.1021/acsapm.9b01079
ACS Appl. Polym. Mater. 2020, 2, 791−804

Scheme 1. Synthesis of the Monomer PAPBZ and the Polymer BAPBZ from Azo-pyridine-2NH$_2$

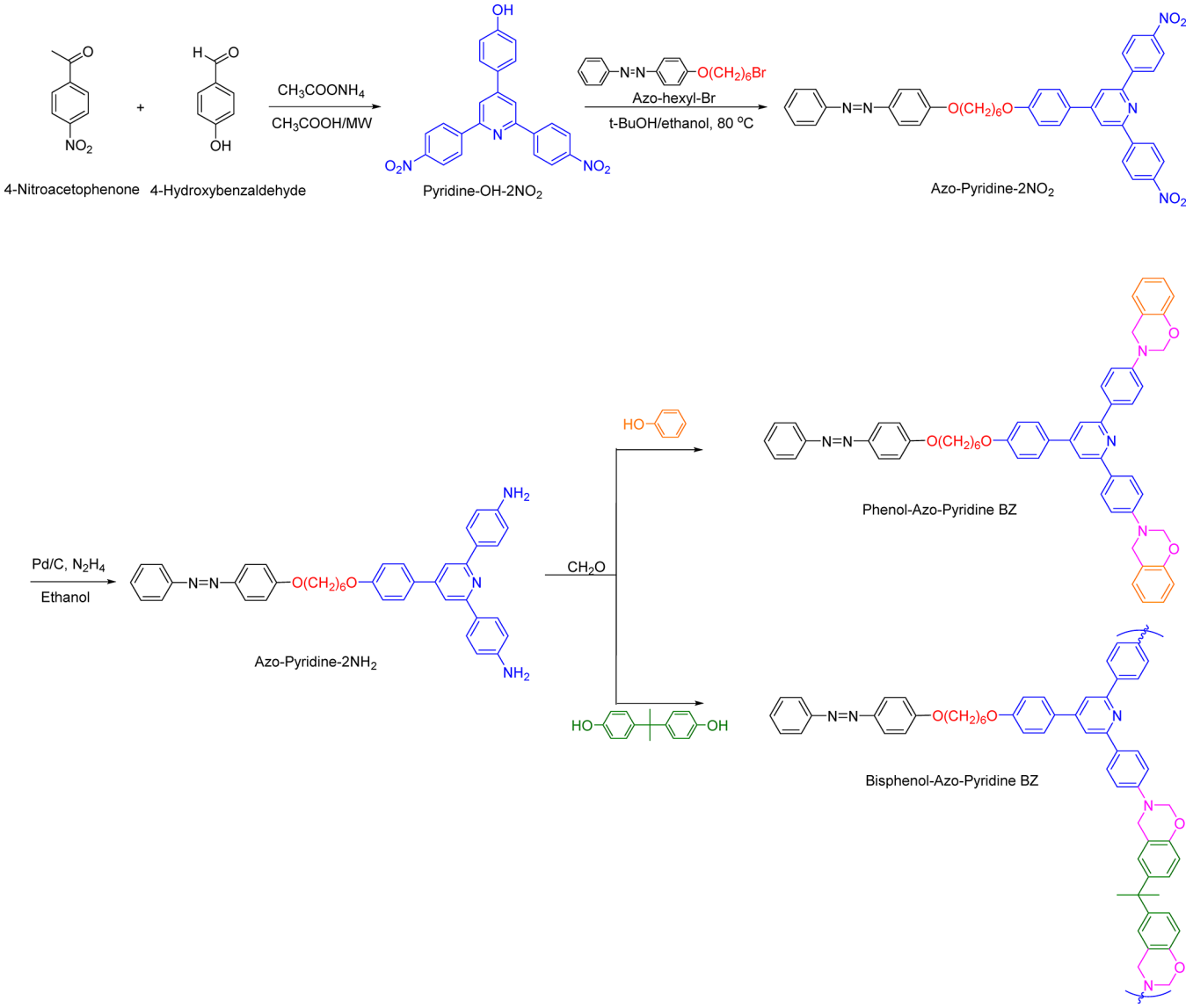

functionalized azobenzene derivative azo-T.[30] Surface relief gratings (SRGs) prepared from the conjugated polymer PTCAz-T and the PVB-DAP/azo-T complex displayed interference patterns with long-range order, suggesting that they might have possible applications in optical storage media. Recently, Yu et al. reported the synthesis of mesomorphic organogel through the self-assembly of oleic acid and azopyridine-containing polymer. Holographic gratings of the resultant organogel were examined and exhibited multiple switching behaviors, which were created by manipulation of the three external stimuli.[31]

Burke et al. reported the first synthesis of a benzoxazine, through the reaction of a p-substituted phenol with formaldehyde and an *N*,*N*-dimethylolamine.[32] Since then, many kinds of benzoxazines have been synthesized, mainly through one-pot Mannich condensations of a wide variety of primary aromatic/aliphatic amines, formaldehyde/paraformaldehyde, and phenol derivatives.[33−35] In addition, various methods have been reported for the incorporation of benzoxazine groups into the skeletons of polymers, including main-chain, side-chain, chain-end, dendrimer, and hyperbranched types.[36−45] Self-cross-linked polymerization of benzoxazine monomers can occur readily through thermal ring opening, without any catalyst, in a process that results in thermosetting polymers having three-dimensional structures, namely, polybenzoxazines.[46,47] Polybenzoxazines have attracted wide-ranging industrial and academic interest because of their low surface energies, low water absorption, excellent electrical properties, high thermal and mechanical stabilities, and low dielectric constants.[48−55] In addition, the highly flexible molecular designs of benzoxazine monomers and their attractive physical and mechanical properties have led to benzoxazine-containing materials receiving much attention for their use in various applications.[52−54,56] Pyridine is a six-membered aromatic heterocycle featuring a lone pair of electrons localized on the nitrogen atom. The incorporation of pyridyl groups into polymers often improves their thermal stability because of the aromaticity and molecular symmetry of these moieties.[57−60] The construction of pyridine-containing polymers typically occurs using pyridine-containing diamines, which can generally be prepared using the Chichibabin reaction or its modification.[61−63] For example, pyridine-

DOI: 10.1021/acsapm.9b01079
ACS Appl. Polym. Mater. 2020, 2, 791−804

Scheme 2. Holographic Setup (a) in the Recording Procedure, (b) in the Reading Procedure, and (c) in Our Study and (d) Appearance of Diffraction Beams with Various Diffraction Orders

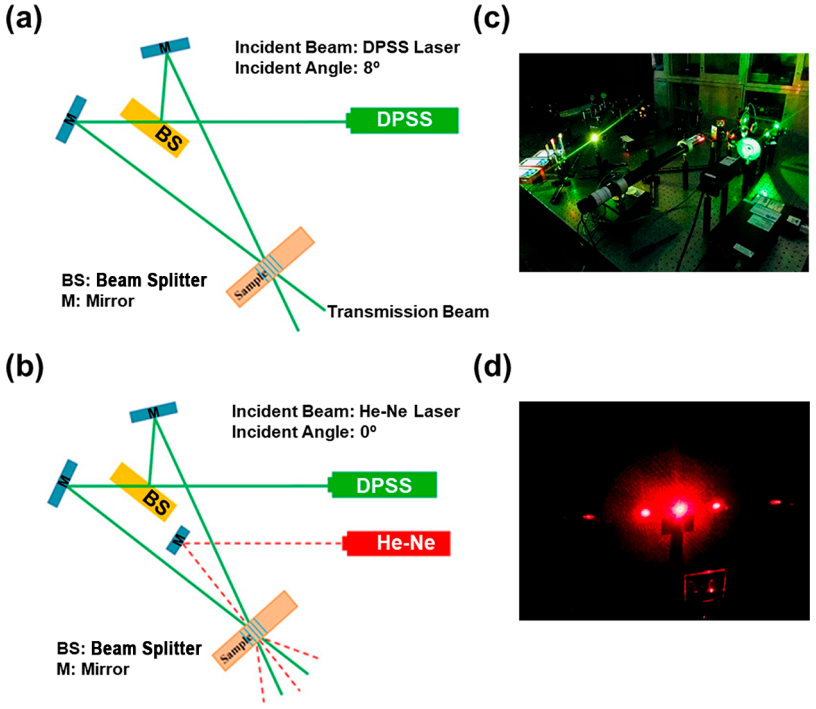

containing polyamides and polyimides prepared using pyridine-containing diamines have exhibited good solubility in polar aprotic solvents, high thermal stability, good flexibility, good mechanical properties, and high dielectric constants.[57−59,64] Recently, pyridine-containing polybenzoxazines have also been reported. Lin et al. prepared a polybenzoxazine featuring pyridine units in its main chain through the Mannich reaction of bisphenol, 4-phenyl-2,6-bis(4-aminophenyl)-pyridine (PNPP), and paraformaldehyde;[36] this polymer exhibited its fluorescence emission at 570 nm upon protonation with HCl, as well as good thermal stability (5% decomposition temperature of up to 414 °C) and a low surface energy (up to 19.6 mJ m^{-2}). They also reported the synthesis of another pyridine-containing polybenzoxazine through the Mannich reaction of phenol, PNPP, and paraformaldehyde. This polybenzoxazine also exhibited good thermal stability (5% decomposition temperature: 396 °C; chair yield: 38%).[65]

From these findings, especially the high thermal stability of polybenzoxazines and pyridine-containing polymers, we were encouraged to examine the combination of a pyridine moiety and a photoresponsive azobenzene moiety within a benzoxazine monomer and a main-chain polybenzoxazine. In this present study, we prepared a new class of azobenzene- and pyridine-functionalized benzoxazines and polybenzoxazines through one-pot Mannich condensations of azo-pyridine-$2NH_2$, paraformaldehyde, and either phenol or bisphenol (Scheme 1). To the best of our knowledge, this paper is the first to describe the incorporation of azobenzene units into thermally stable pyridine-functionalized benzoxazine derivatives and into the main chains of polybenzoxazines, providing new derivatives with tunable thermal properties. We used FTIR and NMR spectroscopy to confirm the chemical structures of the azobenzene- and pyridine-functionalized benzoxazine monomers and their resulting polybenzoxazines. We also used differential scanning calorimetry (DSC) and thermogravimetric analysis (TGA) to investigate the thermal curing behavior and thermal stability of these benzoxazine monomers and their polymers. In addition, we examined the trans-to-cis photoisomerizations of these new materials under UV irradiation and applied them accordingly in the preparation of SRGs.

EXPERIMENTAL SECTION

Materials. 4-Phenylazophenol (98%), 1,6-dibromohexane (97%), potassium carbonate (K_2CO_3), hydrazine hydrate (98%), and bisphenol A (97%) were used as received from Alfa Aesar. Phenol (99%) and paraformaldehyde (96%) were purchased from Sigma−Aldrich. Palladium on carbon (Pd/C, 10 wt %), 1,4-dioxane, *N*,*N*-dimethylformamide (DMF), acetone, and EtOH were obtained from Acros and used as received. The synthesis of 2,6-bis(4-nitrophenyl)-4-(4-((6-(4-(phenyldiazenyl) phenoxy)hexyl)oxy) phenyl)pyridine (azo-pyridine-$2NO_2$) is described in the Supporting Information.

4,4′-(4-(4-((6-(4-(Phenyldiazenyl)phenoxy)hexyl)oxy)-phenyl)pyridine-2,6-diyl)dianiline (Azo-pyridine-$2NH_2$). A solution of azo-pyridine-$2NO_2$ (1.00 g, 0.144 mmol) and Pd/C (10 wt %, 60 mg) in EtOH (80 mL) was placed in a 100 mL flask and stirred under a N_2 atmosphere at 90 °C. Hydrazine hydrate (3 mL) was added portionwise to the mixture, which was then stirred at 90 °C for 48 h. The mixture was filtered while hot and washed with EtOH. After cooling, the precipitate was filtered off and washed with EtOH. The precipitate was dried overnight at 50 °C under vacuum to give a yellow powder. Yield: 82%; FTIR (KBr, cm^{-1}): 3452 (amino group), 3363 (amino group), 3039 (aromatic CH), 2935 (aliphatic CH), 2858 (aliphatic CH), 1620 (phenyl ring), 1599 (NH stretching), 1512 (phenyl ring), 1438 (N═N stretching). ^{1}H NMR (DMSO-d_6, 600 MHz, ppm): δ = 7.98 (d, J = 7.8 Hz, 4H), 7.88 (d, J = 10.8 Hz, 4H), 7.82 (d, J = 9.6 Hz, 2H), 7.75 (s, 2H), 7.56 (t, J = 10.8 Hz, 2H), 7.32 (t, J = 9 Hz, 1H), 7.12 (d, J = 10.8 Hz, 2H), 7.05 (d, J = 10.2 Hz, 2H), 6.66 (d, J = 7.8 Hz, 4H), 5.40 (s, 2H, NH_2), 4.09 (t, J = 7.2 Hz, 4H, OCH_2), 1.78 (t, J = 5.4 Hz, 4H), 1.51 (t, J = 5.4 Hz, 4H). ^{13}C NMR (DMSO-d_6, 125 MHz, ppm): δ = 161.52 (aromatic CO), 159.34 (aromatic CO), 156.47 (pyridine C═N), 152.01 (aromatic N═NC), 149.79 (aromatic CNH_2), 148.07 (aromatic CN═N),

DOI: 10.1021/acsapm.9b01079
ACS Appl. Polym. Mater. 2020, 2, 791−804

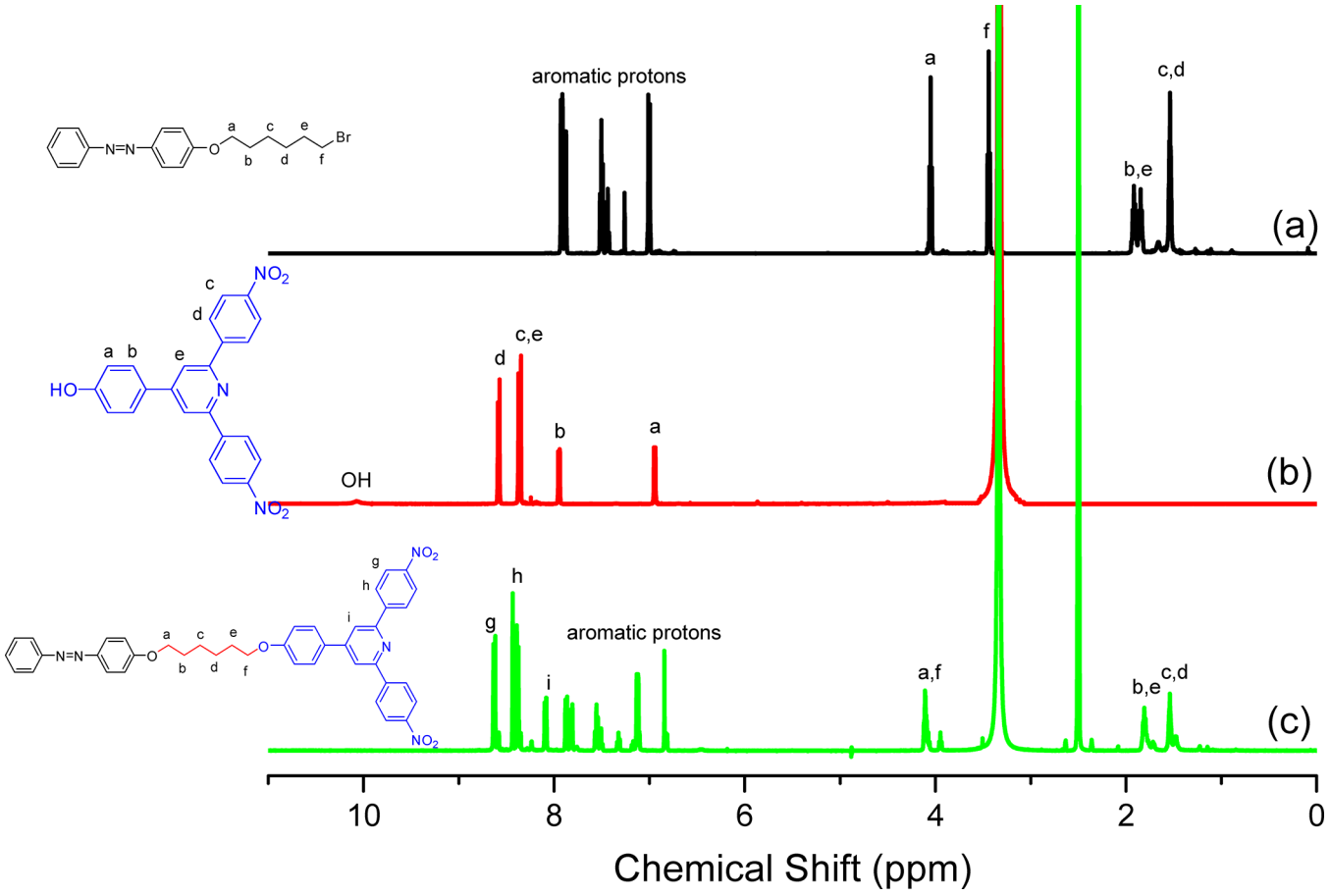

Figure 1. ^{1}H NMR spectra of (a) azo-hexyl-Br, (b) pyridine-OH-2NO_2, and (c) azo-pyridine-2NO_2.

146.03 (aromatic CN═N), 130.79 (aromatic C), 130.49 (aromatic C), 129.38 (aromatic CH), 129.10−112.08 (aromatic CH), 67.96 (OCH_2), 28.62 (CH_2), 25.29 (CH_2).

3,3′-((4-(4-((6-(4-(Phenyldiazenyl)phenoxy)hexyl)oxy)-phenyl)pyridine-2,6-diyl)bis(4,1-phenyl-ene))bis(3,4-dihydro-2*H*-benzo[*e*][1,3]oxazine) (Phenol-azo-pyridine BZ, PAPBZ). A solution of azo-pyridine-2NH_2 (0.750 g, 1.18 mmol) and phenol (0.334 g, 3.55 mmol) in toluene/EtOH (2:1, 10 mL) was added portionwise to a solution of paraformaldehyde (0.213 g, 7.10 mmol) in toluene/EtOH (2:1, 30 mL) in a 50 mL flask. The mixture was stirred overnight under N_2 at 90 °C. After cooling and rotary evaporation, the residue was dried at 50 °C under vacuum for 24 h to give an orange gel, which was purified through column chromatography [eluent: tetrahydrofuran (THF)/hexane, 1:1]. Yield 70%; FTIR (KBr, cm^{-1}): 3037 (aromatic CH), 2925 (aliphatic CH), 2854 (aliphatic CH), 1606 (phenyl ring), 1510 (phenyl ring), 1429 (N═N stretching), 1233 (benzoxazine), 928 (benzoxazine). ^{1}H NMR (DMSO-d_6, 600 MHz, ppm): δ = 8.14−6.74 (m, aromatic CH), 5.52 (s, 4H, OCH_2N), 4.73 (s, 4H, CH_2N), 4.04 (t, J = 7.8 Hz, 4H, OCH_2), 1.74 (t, J = 3.6 Hz, 4H), 1.50 (t, J = 3.6 Hz, 4H). ^{13}C NMR (DMSO-d_6, 125 MHz, ppm): δ = 161.50−139.18 (aromatic C), 129.35−114.99 (aromatic CH), 78.17 (OCH_2N), 67.93 (OCH_2), 67.51 (CH_2N), 67.01 (OCH_2), 28.54 (CH_2), 25.12 (CH_2).

Poly(4-(2-(3-(4-(6-phenyl-4-(4-((6-(4-(phenyldiazenyl)-phenoxy)hexyl)oxy)phenyl)pyrid-2-yl)phenyl)-3,4-dihydro-2*H*-benzo[*e*][1,3]oxazin-6-yl)propan-2-yl)3,4-dihydro-2*H*-benzo[*e*][1,3]oxazine (Bisphenol-azo-pyridine BZ, BAPBZ). A solution of azo-pyridine-2NH_2 (0.750 g, 1.18 mmol) and bisphenol A (0.270 g, 1.18 mmol) in toluene/EtOH (1:1, 10 mL) was added portionwise to a solution of paraformaldehyde (0.143 g, 4.80 mmol) in toluene/EtOH (1:1, 30 mL). The mixture was stirred overnight under N_2 at 90 °C. After cooling and rotary evaporation, the residue was dried at 50 °C under vacuum for 24 h to give a yellow solid, which was purified through column chromatography (eluent: THF/hexane, 1:1). Yield 75%; FTIR (KBr, cm^{-1}): 3041 (aromatic CH), 2931 (aliphatic CH), 2858 (aliphatic CH), 1606 (phenyl ring), 1510 (phenyl ring), 1431 (N═N stretching), 1233 (benzoxazine), 928 (benzoxazine). ^{1}H NMR ($CDCl_3$, 600 MHz, ppm): δ = 8.03−6.74 (m, aromatic CH), 5.36 (br d, OCH_2N), 4.75 (br d, CH_2N), 4.07 (t, J = 7.2 Hz, 4H, OCH_2), 1.60 (m, CH_3), 1.25 (m, 4H), 1.11 (s, 4H). ^{13}C NMR ($CDCl_3$, 125 MHz, ppm): δ = 161.58−142.69 (aromatic C), 130.29−114.66 (aromatic CH), 78.66 (OCH_2N), 68.12 (CH_2N), 67.91 (OCH_2), 41.67 (OCH_2), 31.03 (CH_3), 29.09 (CH_2), 25.82 (CH_2).

Photocontrollable Thin Films. A glass test piece having a length and width of 2.5 cm × 2.5 cm and a thickness of 1 mm was cleaned ultrasonically through sequential immersion in THF, acetone, and a neutral detergent. After drying this substrate, a small amount of the sample solution was coated onto its surface through drop-coating; the substrate was placed on a hot plate and heated at 40 °C until the solvent had completely evaporated, providing a homogeneous thin film.

SRGs. Thin films of PAPBZ and BAPBZ were prepared as described above. Polarized green light (wavelength: 532 nm; intensity: 20 mW cm^{-2}) was generated from a diode-pumped solid-state laser. The scattered laser light was collimated and then passed through a polarized beam splitter. An incident angle of 8° for the reference beam was maintained in air, as outlined in Scheme 2. A transverse-electric polarized (TEP) He−Ne laser beam (wavelength: 623 nm) was applied to probe the grating.

RESULTS AND DISCUSSION

Preparation of the PAPBZ Monomer and the BAPBZ Polymer. For this study, our objective was to incorporate azo-dye units into pyridine-based benzoxazine moieties and into

DOI: 10.1021/acsapm.9b01079
ACS Appl. Polym. Mater. 2020, 2, 791−804

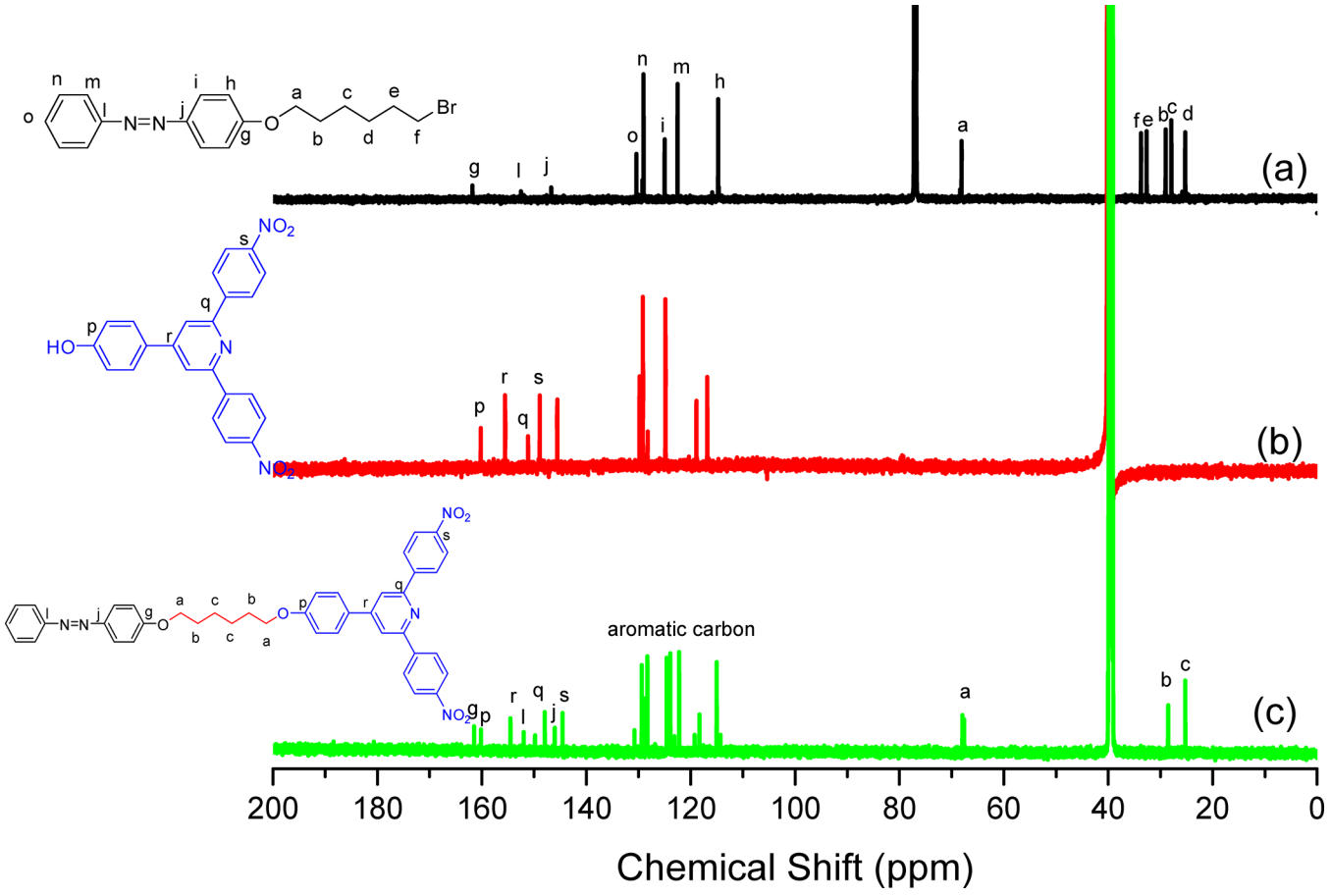

Figure 2. ^{13}C NMR spectra of (a) azo-hexyl-Br, (b) pyridine-OH-2NO_2, and (c) azo-pyridine-2NO_2.

the main chains of pyridine-based polybenzoxazines and then to examine their photocontrollable behavior through photo-induced trans-to-cis isomerization. The preparation of the PAPBZ monomer and the BAPBZ polymer occurred in two stages: the synthesis of the starting diamino precursor azo-pyridine-2NH_2 and then its use in the preparation of the desired azo monomers and polymers. We prepared the azo-pyridine-2NH_2 precursor in three steps (Scheme 1). First, a Chichibabin reaction of 4-nitroacetophenone, 4-hydroxybenzaldehyde, and ammonium acetate in acetic acid under microwave conditions afforded pyridine-OH-2NO_2 in good yield. Second, azo-pyridine-2NO_2 was produced through O-alkylation of pyridine-OH-2NO_2 with azo-hexyl-Br in dry EtOH in the presence of *t*-BuOH at 80 °C for 24 h. Azo-hexyl-Br itself was synthesized through O-alkylation of 4-phenylazophenol with 1,6-dibromohexane in acetone in the presence of K_2CO_3 at 80 °C overnight. Finally, the catalytic reduction of azo-pyridine-2NO_2 mediated by hydrazine hydrate in dry EtOH in the presence of 10% Pd/C at 90 °C for 48 h afforded azo-pyridine-2NH_2 in excellent yield. Subsequently, the monomer PAPBZ was synthesized through the one-pot Mannich reaction of azo-pyridine-2NH_2, paraformaldehyde, and phenol in toluene and EtOH (2:1) at 90 °C overnight; the polymer BAPBZ was also prepared through the one-pot Mannich reaction of azo-pyridine-2NH_2, paraformaldehyde, and bisphenol A in toluene and EtOH (1:1) at 90 °C overnight.

The chemical structures of azo-hexyl-Br, pyridine-OH-2NO_2, and azo-pyridine-2NO_2 were confirmed through FTIR and NMR spectroscopic analyses. The FTIR spectrum of azo-hexyl-Br (Figure S1) exhibited strong aliphatic signals in the range of 2939−2862 cm^{-1}, a sharp signal at 1462 cm^{-1} corresponding to the azo (N═N) group, and a signal at 1257 cm^{-1} corresponding to the stretching vibration of the C−N unit. The spectrum of pyridine-OH-2NO_2 (Figure S2) featured four signals: at 3469 cm^{-1} for the OH unit, at 3076 cm^{-1} for the stretching of the aromatic C−H unit, at 1516 cm^{-1} for the nitro (NO_2) groups, and at 1346 cm^{-1} for the C−N groups. The FTIR spectrum of azo-pyridine-2NO_2 (Figure S3) exhibited a signal for stretching of the aromatic unit at 3070 cm^{-1}, signals for stretching of the aliphatic units in the range of 2937−2858 cm^{-1}, and signals at 1519, 1440, and 1338 cm^{-1} representing the nitro (NO_2), azo (N═N), and C−N groups, respectively. Figure 1 presents the ^1H NMR spectra of azo-hexyl-Br, pyridine-OH-2NO_2, and azo-pyridine-2NO_2. The ^1H NMR spectrum of azo-hexyl-Br (Figure 1a) exhibited signals at 4.05, 3.44, 1.91, and 1.54 ppm representing the OCH_2, CH_2Br, $2CH_2$, and $2CH_2$ units, as well as signals in the range of 7.91−7.01 ppm for the aromatic protons. The ^1H NMR spectrum of pyridine-OH-2NO_2 (Figure 1b) was characterized by signals for the OH group and its aromatic protons at 10.07 and 8.59−6.95 ppm, respectively. The spectrum of azo-pyridine-2NO_2 (Figure 1c) featured signals for its aromatic protons from 8.62 to 6.84 ppm, as well as signals for its aliphatic protons from 4.11 to 1.54 ppm. ^{13}C NMR spectroscopy confirmed the chemical structures of azo-hexyl-Br, pyridine-OH-2NO_2, and azo-pyridine-2NO_2.

DOI: 10.1021/acsapm.9b01079
ACS Appl. Polym. Mater. 2020, 2, 791−804

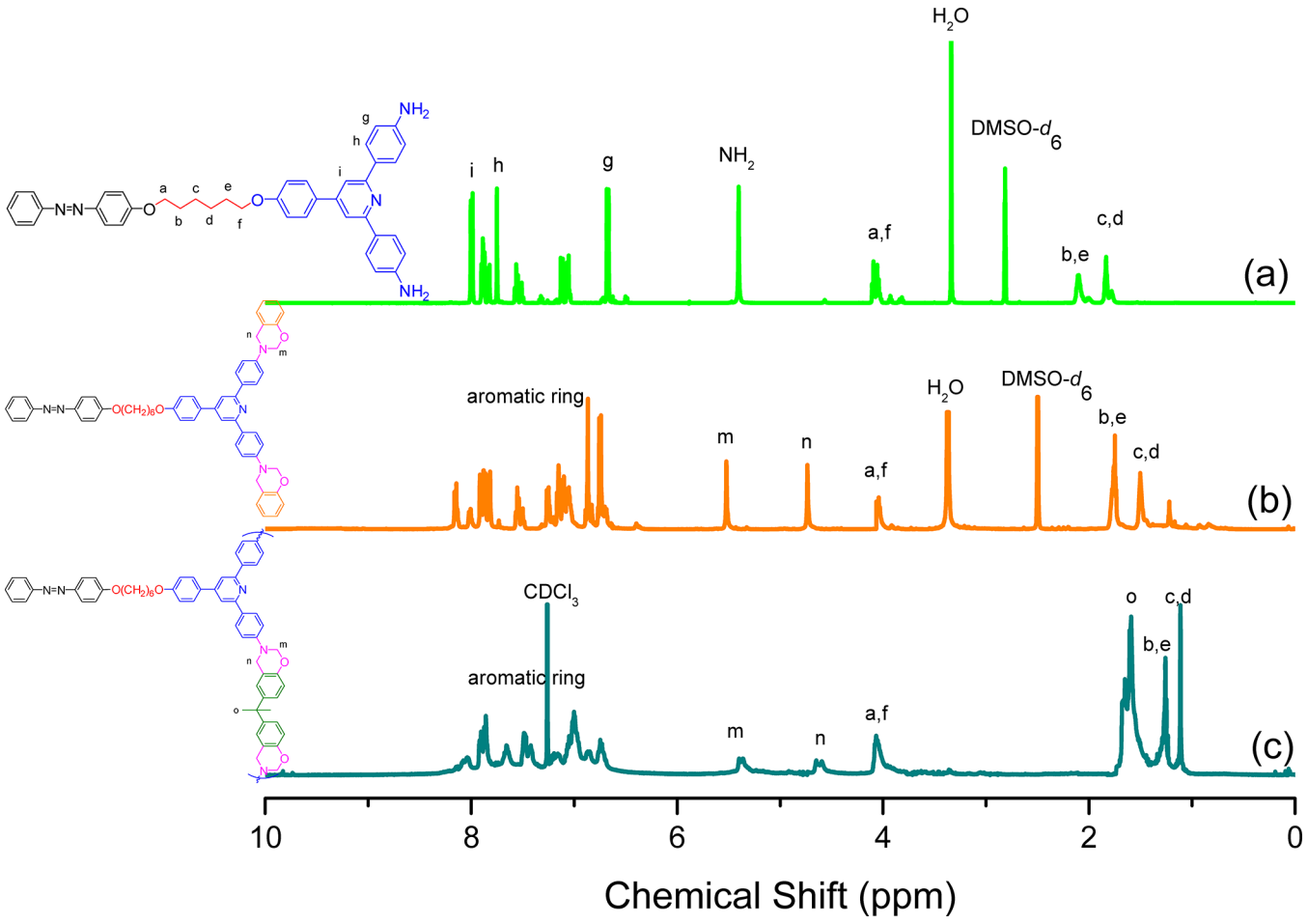

Figure 3. ^{1}H NMR spectra of (a) azo-pyridine-2NH$_2$, (b) the monomer PAPBZ, and (c) the polymer BAPBZ.

Figure 2a presents the ^{13}C NMR spectrum of azo-hexyl-Br, revealing signals at 68.11 and 33.73 ppm for its OCH_2 and CH_2Br units, respectively; signals for its other aliphatic carbon nuclei in the range of 32.64−25.26 ppm; and signals for its aromatic carbon nuclei in the range of 161.78−114.73 ppm. The ^{13}C NMR spectrum of pyridine-OH-2NO$_2$ (Figure 2b) exhibited signals at 159.38, 154.73, 150.30, and 148.13 ppm for its COH, pyridine C═N, pyridine C, and C−NO$_2$ carbon nuclei, respectively, in addition to signals for its other aromatic carbon nuclei in the range of 150.30−116.22 ppm. The ^{13}C NMR spectrum of azo-pyridine-2NO$_2$ (Figure 2c) possessed four characteristic signals at 151.99, 147.93, 146.02, and 144.55 ppm for its N═N−C, pyridine C═N, C−N═N, and C−NO$_2$ carbon nuclei, respectively; signals for its aromatic and aliphatic carbon nuclei appeared in the ranges of 130.78−114.27 and 67.93−25.24 ppm, respectively.

We used FTIR spectroscopy and ^{1}H and ^{13}C NMR spectroscopy to confirm the chemical structures of the diamino precursor azo-pyridine-2NH$_2$, the monomer PAPBZ, and the polymer BAPBZ; we also used gel permeation chromatography (GPC) to characterize this polymer. Figure 3 presents the FTIR spectra of azo-pyridine-2NH$_2$, the PAPBZ monomer, and the BAPBZ polymer. The spectrum of azo-pyridine-2NH$_2$ (Figure S4a) featured signals at 3452 and 3363 cm^{-1} for symmetric and asymmetric NH$_2$ stretching; at 2935 and 2858 cm^{-1} for aliphatic stretching; and at 1599 and 1438 cm^{-1} for the stretching vibrations of the N−H and azo N═N units. The spectra of the PAPBZ monomer and the BAPBZ polymer (Figure S4b,c) featured signals at 2925−2854 and 2931−2858 cm^{-1} for the stretching of aliphatic groups, in addition to signals at 1429 and 1431 cm^{-1} representing their respective azo (N═N) groups. Benzoxazine formation for both the monomer and polymer was confirmed by the presence of signals for asymmetric oxazine and trisubstituted benzene units at 928 and 1510 cm^{-1} for PAPBZ and at 924 and 1510 cm^{-1} for BAPBZ. Moreover, benzoxazine formation was also evidenced by the appearance of signals for asymmetric Ar−O−C stretching at 1233 cm^{-1} for PAPBZ and at 1233 cm^{-1} for BAPBZ.

Figure 3a presents the ^{1}H NMR spectrum of azo-pyridine-2NH$_2$, featuring a strong signal at 5.40 ppm for the two amino (NH$_2$) protons, as well as signals for the aromatic and aliphatic protons at 7.98−6.66 and 4.09−1.51 ppm, respectively. Benzoxazine formation in PAPBZ and BAPBZ was confirmed using ^{1}H NMR spectroscopy, as outlined in Figure 3b,c. The characteristic signals at 5.52 (OCH_2N) and 4.73 ($ArCH_2N$) ppm for PAPBZ and at 5.52 (OCH_2N) and 4.73 ($ArCH_2N$) ppm for BAPBZ revealed the presence of benzoxazine rings. No signal characteristic of a NCH_2Ar unit was evident near 4.00 ppm, as would have been produced through ring opening of the benzoxazine units. The close integration ratio (1:1) of the signals at 5.52 and 4.73 ppm for PAPBZ and of the signals at 5.52 and 4.73 ppm for BAPBZ confirmed the high purity of our synthesized samples.

Figure 4a presents the ^{13}C NMR spectrum of azo-pyridine-2NH$_2$, featuring signals at 156.47 and 149.79 ppm for the

DOI: 10.1021/acsapm.9b01079
ACS Appl. Polym. Mater. 2020, 2, 791−804

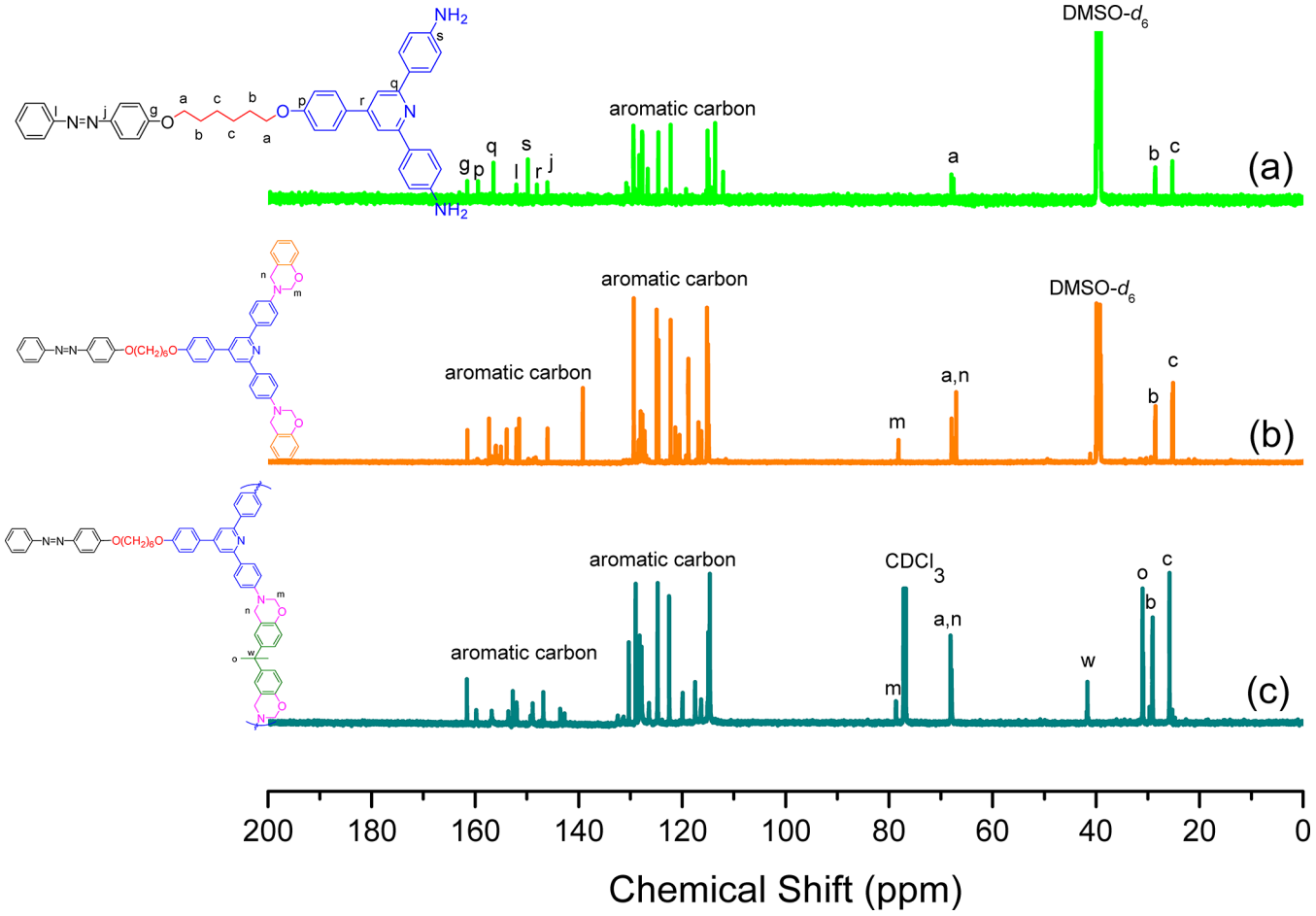

Figure 4. ^{13}C NMR spectra of (a) azo-pyridine-2NH_2, (b) the monomer PAPBZ, and (c) the polymer BAPBZ.

pyridine C═N and aromatic C−NH_2 carbon nuclei, respectively, as well as signals for the aliphatic carbon nuclei at 67.96, 28.62, and 25.29 ppm. As observed in Figure 4b,c, the signals for the carbon nuclei of the OCH_2N and $ArCH_2N$ moieties of the benzoxazine units appeared at 78.17 and 67.93 ppm for PAPBZ and at 78.66 and 68.12 ppm for BAPBZ; the signals of the other aliphatic and aromatic carbon nuclei appeared at their expected chemical shifts. All of these spectroscopic data confirmed the preparation of the target benzoxazine monomer and polymer containing azo and pyridine moieties. Furthermore, we applied GPC analysis to estimate the molecular weight of the polymer BAPBZ; its number-average molecular weight (M_n) was 1590 g mol^{-1}, and its polydispersity index (PDI) was 1.23.

Ring-Opening Polymerization (ROP) of the PAPBZ Monomer and the BAPBZ Polymer. To investigate the thermal ROP and curing behavior of these pyridine-based benzoxazine derivatives containing azo units, we used DSC and FTIR spectroscopy to monitor the thermal changes of the monomer PAPBZ and the polymer BAPBZ. Figure 5a presents the DSC thermograms of the PAPBZ monomer at various curing stages. The DSC thermogram of the noncured PAPBZ monomer featured two exothermic peaks—one at 236 °C with a polymerization heat of 165.9 J g^{-1} and another at 310 °C with a polymerization heat of 96.8 J g^{-1}. We attribute the appearance of two exothermic peaks to the self-catalytic behavior of the pyridine moiety, which contributed to decrease the polymerization temperature from 310 to 236 °C.

Shibayama et al. prepared a pyridyl-containing benzoxazine derivative (B-3py) through a Mannich reaction of 3-aminopyridine, paraformaldehyde, and bisphenol A; they found that the exothermal peak accompanying the ROP of B-3py shifted to lower temperature because the pyridyl unit acted as a basic catalyst for the ROP.[66] In addition, they reported that the zwitterionic intermediate that formed upon ring opening of B-3py was stabilized by the lone pair of electrons of the pyridyl unit, thereby accelerating the ROP at lower temperature. Lin et al. confirmed this catalytic behavior of the pyridyl unit;[36,65] they prepared a pyridyl-containing benzoxazine and compared its polymerization heat with that of a structurally similar benzoxazine derivative, with the pyridyl ring replaced by a benzene ring (phenyl-containing benzoxazine). They observed that the polymerization heat of the pyridyl-containing benzoxazine was lower than that of the phenyl-containing benzoxazine, indicating the catalytic behavior of the pyridyl unit. Our present results are consistent with these previous reports and confirm the basic catalytic behavior of the pyridyl group. We found that the enthalpies of the exotherms of PAPBZ gradually decreased upon increasing the curing and ring-opening temperatures, while the maximum exothermic temperatures increased. Upon increasing the curing temperature from 180 to 210 to 240 °C, the enthalpy decreased from 95.6 to 52.2 to 5.0 J g^{-1}, and the maximum exothermic temperature increased from 307 to 312 to 330 °C. The exothermic peak of PAPBZ disappeared completely after applying a curing temperature of 270 °C or higher, implying

DOI: 10.1021/acsapm.9b01079
ACS Appl. Polym. Mater. 2020, 2, 791−804

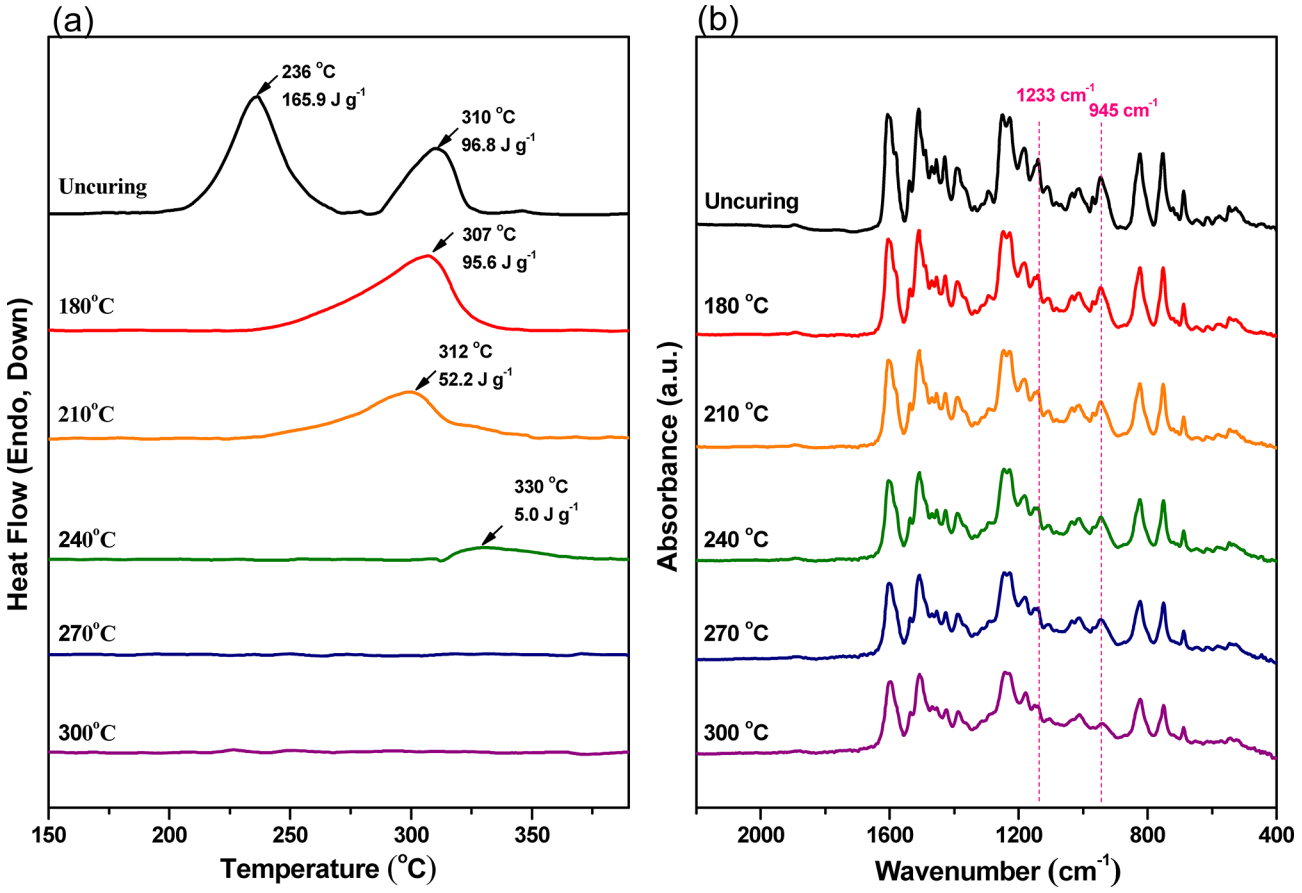

Figure 5. (a) DSC thermograms and (b) FTIR spectra of the monomer PAPBZ after each heating stage.

that suitable temperatures for ring opening of the benzoxazine unit and thermal polymerization of PAPBZ were above 240 °C. Figure 5b presents FTIR spectra of PAPBZ recorded before and after various stages of curing; we monitored the characteristic absorption signals for asymmetric C−O−C stretching at 1233 cm^{-1} and for the oxazine ring at 928 cm^{-1}. Progressive decreases in the adsorption intensities of these peaks occurred upon increasing the curing temperature from 180 to 240 °C. After curing at 240 °C, the signals at 1233 and 928 cm^{-1}, characterizing the benzoxazine ring, had disappeared, confirming that the temperature for thermal ROP of PAPBZ was 240 °C or above. These findings were consistent with those obtained through the DSC analyses.

Similarly, we also used DSC and FTIR to investigate the thermal ring opening and cross-linking of the BAPBZ polymer. Figure 6a presents DSC traces of the BAPBZ polymer after its curing at various stages. The thermogram of the noncured BAPBZ featured a single exothermic peak at 279 °C with a polymerization heat of 227.9 J g^{-1}. The exothermic enthalpies of BAPBZ decreased progressively upon increasing the curing temperature. Thermal curing of BAPBZ to produce its cross-linked products at 180, 210, 240, and 270 °C resulted in increases in the resulting maximum exothermic temperatures to 281, 309, 345, and 358 °C, respectively, along with decreases in the cross-linking heats to 160.9, 106.6, 45.0, and 28.9 J g^{-1}, respectively. Applying a curing temperature of 300 °C resulted in complete disappearance of the exothermic peak, indicating that the temperature required for the cross-linking and ROP of the benzoxazine units of the polymer BAPBZ was 300 °C or above. We also performed FTIR spectral analyses after various stages of curing to investigate the thermal cross-linking polymerization and ROP of the BAPBZ polymer. As displayed in Figure 6b, the absorption intensities of the signals of the benzoxazine rings—for its asymmetric C−O−C stretching at 1233 cm^{-1} and for its oxazine ring at 924 cm^{-1}—decreased gradually upon increasing the curing temperature from 180 to 270 °C. Total disappearance of these signals occurred when the thermal curing temperature was 300 °C. Thus, these spectral findings were consistent with the DSC data and indicated that the optimal temperature for ring opening of the benzoxazine units in the polymer BAPBZ and for the formation of a high-density cross-linked polymer was 300 °C.

TGA of Phenol-azo-pyridine Bz and Bisphenol-azo-pyridine Bz. We used TGA to investigate the thermal stability of PAPBZ and BAPBZ. Figure 7a presents TGA thermograms of PAPBZ prior to curing and after curing at various temperatures. The 10% degradation temperature (T_{d10}) and char yield at 800 °C both increased upon increasing the curing temperature. We attribute this thermal behavior to ROP of the benzoxazine rings. The uncured PAPBZ provided a value of T_{d10} of 339 °C, with a char yield at 800 °C of 45%. The values of T_{d10} increased to 389, 400, 407, 426, and 443 °C (with char yields of 46, 47, 50, 51, and 51%, respectively) when the curing temperature increased to 180, 210, 240, 270, and 300 °C, respectively. Interestingly, the derivative weight loss thermogram (Figure 7b) of the noncured BAPBZ featured two stages of weight loss: one in the range of 272−357 °C, which corresponded to ROP of the benzoxazine rings, and another in the range of 423−551 °C, which was presumably caused by

DOI: 10.1021/acsapm.9b01079
ACS Appl. Polym. Mater. 2020, 2, 791−804

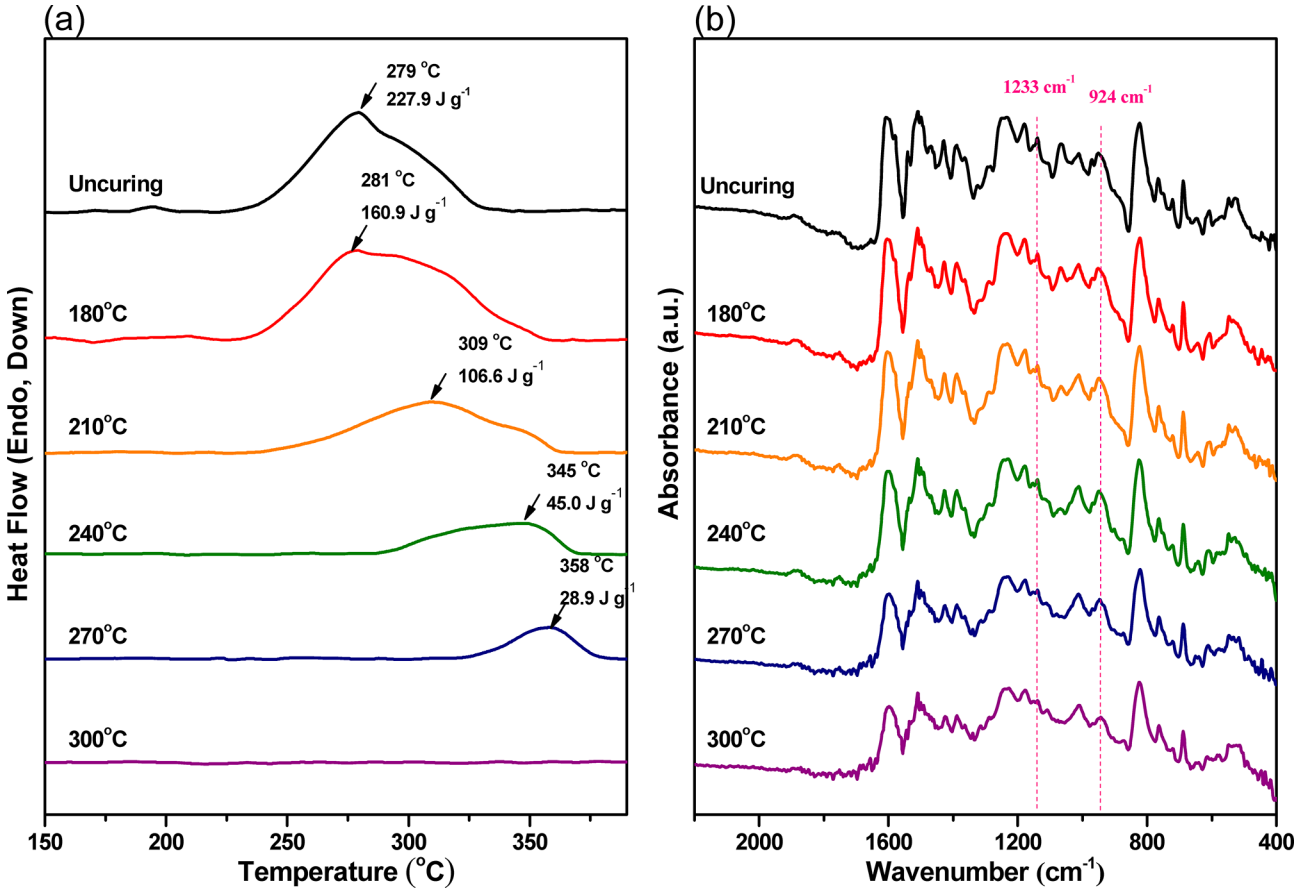

Figure 6. (a) DSC thermograms and (b) FTIR spectra of the polymer BAPBZ after each heating stage.

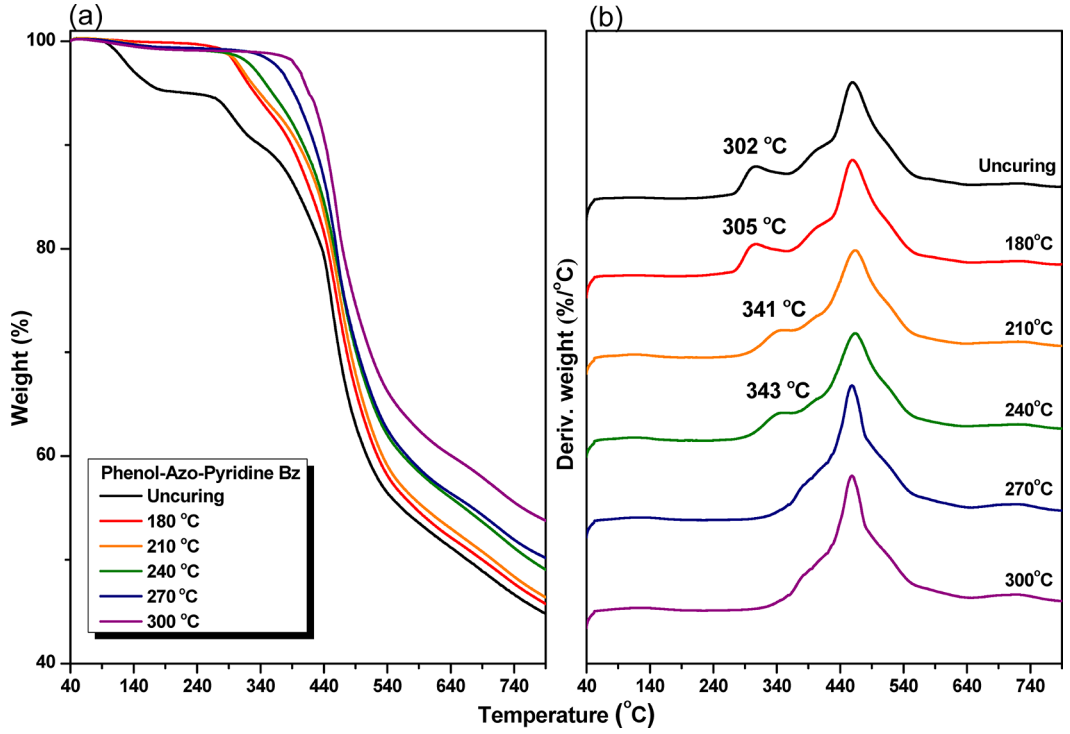

Figure 7. (a) TGA and (b) derivative weight loss thermograms of the monomer PAPBZ after each heating stage.

decomposition of other units. The first weight loss stage, corresponding to ROP of the benzoxazine rings, shifted to higher temperature upon increasing the curing temperature. The maximum temperature of the first weight loss stage (T_1) shifted to 305, 341, and 343 °C after curing at temperatures of 180, 210, and 240 °C, respectively (cf. a maximum

DOI: 10.1021/acsapm.9b01079
ACS Appl. Polym. Mater. 2020, 2, 791−804

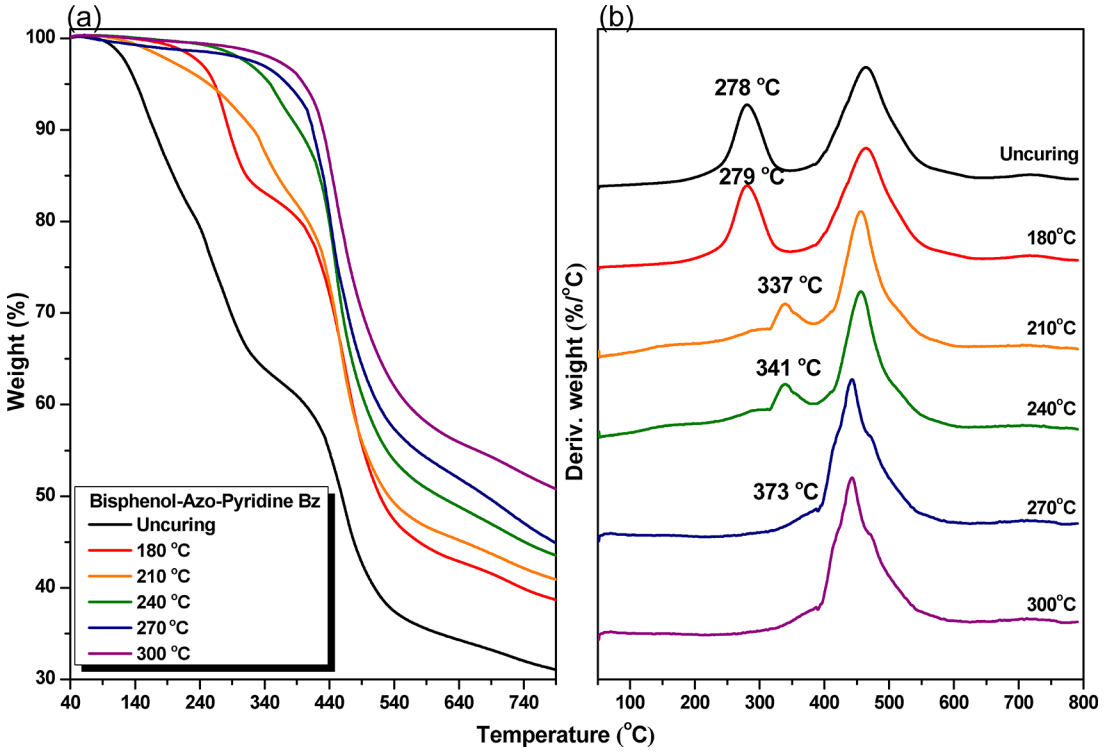

Figure 8. (a) TGA and (b) derivative weight loss thermograms of the polymer BAPBZ after each heating stage.

temperature of 302 °C for the noncured PAPBZ). This weight loss stage disappeared completely after thermal curing at a temperature of 270 °C, indicating that the optimal temperature for ROP of the benzoxazine ring was above 240 °C. These findings were consistent with those obtained using DSC and FTIR spectroscopy (Figure 5).

Figure 8 presents TGA thermograms of BAPBZ before and after curing at various stages. Within Figure 8a, the value of T_{d10} and the char yield increased upon increasing the curing temperature; we attribute this behavior to the ring opening of the benzoxazine rings and the cross-linking of the BAPBZ polymer. The value of T_{d10} and the char yield of the noncured BAPBZ were 169 °C and 31%, respectively. When the curing temperature increased to 180, 210, 240, 270, and 300 °C, the value of T_{d10} increased to 284, 322, 393, 414, and 429 °C, respectively, and the char yield increased to 39, 40, 44, 45, and 50%, respectively. In addition, the derivative weight loss thermogram of the noncured BAPBZ featured (Figure 8b) two weight loss stages: one in the range of 223−332 °C, corresponding to ROP of the benzoxazine rings and cross-linking of the BAPBZ polymer, and the other in the range of 380−550 °C, which we attribute to decomposition of other units. The maximum temperature of the first weight loss stage shifted to higher temperature upon increasing the curing temperature, appearing at 279, 337, 341, and 373 °C after curing at 180, 210, 240, and 270 °C, respectively. This first weight loss stage disappeared completely after thermal curing at 300 °C, indicating that the optimal temperature for ring opening of the benzoxazine rings and cross-linking of the BAPBZ polymer was 300 °C. These TGA findings are consistent with those obtained from the DSC and FTIR spectroscopic analyses (Figure 6).

Photoresponsivity of the Azobenzene-Containing Monomer PAPBZ and Polymer BAPBZ. Azobenzenes typically undergo reversible trans-to-cis photoisomerizations when irradiated with UV light.[28,67] We investigated the photoresponsivities of the monomer PAPBZ and the polymer BAPBZ by measuring the UV−Vis spectra of their DMF solutions before and after UV light irradiation at a wavelength of 365 nm and then continued recording their spectra until the photostationary states of the monomer and polymer had been attained. Figure 9 reveals that the intensities of the UV absorptions at 386 nm for PAPBZ (Figure 9c) and at 378 nm for BAPBZ (Figure 9e), corresponding to $\pi-\pi^*$ transitions, gradually decreased, while the intensities of the UV absorptions at 439 nm for PAPBZ (Figure 9d) and at 440 nm for BAPBZ (Figure 9f), corresponding to $n-\pi^*$ transitions, gradually increased upon their trans-to-cis isomerizations under UV irradiation. The absorption at 280 nm for both PAPBZ and BAPBZ corresponded to the $\pi-\pi^*$ transitions in the conjugated system of triphenyl pyridine moieties. The trans isomers of both PAPBZ and BAPBZ were transformed completely into their cis isomers after 30 min of UV irradiation; placing them in the dark for 24 h caused their cis isomers to revert back to their original trans isomers. A slow cis-to-trans photoisomerization and a rapid trans-to-cis photoisomerization are typical of azobenzene-containing compounds.[68] We calculated the degree of trans-to-cis photoisomerization (η) using the equation

$$\eta = 1 - (A_s/A_0)$$

A_0 and A_s are the intensities of the absorptions at a wavelength of 439 nm for the photopristine and photostationary states, respectively. The degrees of isomerization of PAPBZ and BAPBZ were 19.3 and 13.9%, respectively. This is compared with our previously reported azide- and azobenzene-functionalized (PTCAz-N_3) and thymine- and azobenzene-functionalized (PTCAz-T) conjugated copolymers, which exhibited degrees of isomerization of 26.3 and 26.7%.[29] The relative low of degree of isomerization of the synthesized PAPBZ and

DOI: 10.1021/acsapm.9b01079
ACS Appl. Polym. Mater. 2020, 2, 791−804

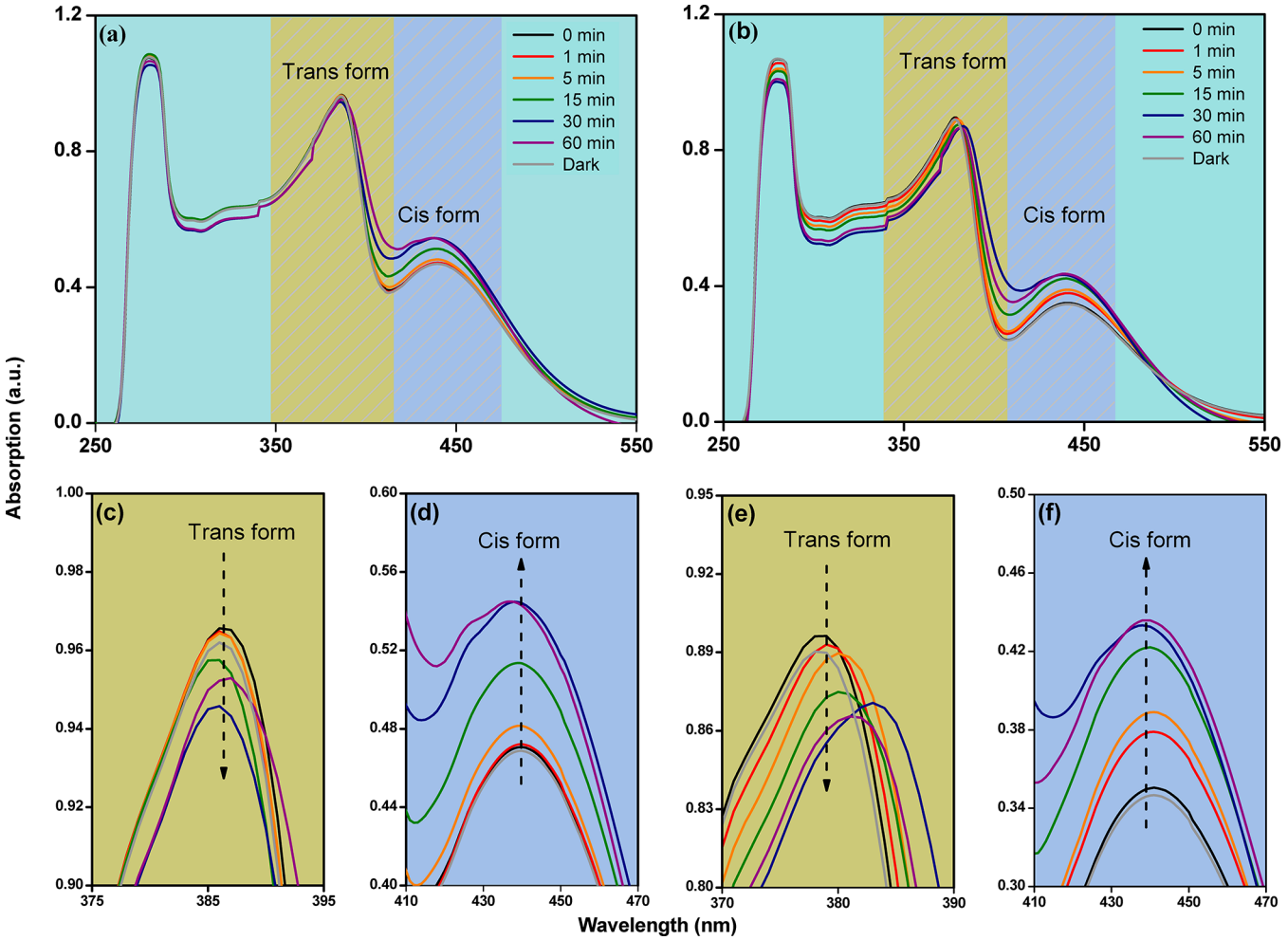

Figure 9. (a,b) UV−vis spectra of (a) the monomer PAPBZ and (b) the polymer BAPBZ before and after irradiation with a UV lamp at a wavelength of 365 nm for various times (0−60 min) and after placing in the dark for 24 h. (c−f) Magnified regions of the spectra of the trans (c,e) and cis (d,f) isomers of (c,d) PAPBZ and (e,f) BAPBZ.

BAPBZ could be attributed to the high cross-linking and rigid nature of polybenzoxazines, which restricted the conversion of azobenzene from trans to cis.

Photoinduced SRGs Fabricated from the PAPBZ Monomer and the BAPBZ Polymer. We deposited transparent films of various thicknesses of the azobenzene-containing monomer PAPBZ and polymer BAPBZ through spin-coating onto glass substrates to fabricate SRGs, as displayed in Scheme 2. Figure 10 presents the diffraction efficiencies of these systems as well as atomic force microscopy (AFM) images. The films of the azobenzene-containing monomer PAPBZ and polymer BAPBZ exhibited obvious spots after illumination with a polarized green laser, suggesting that their refractive indices had changed. Strong second-order diffraction spots appeared, observed with one-dimensional diffraction, for the azobenzene-containing monomer PAPBZ after grating formation, as displayed in Scheme 2d. The grating spatial period of each sample tested in this study was approximately 1.85 μm, with surface-modulation depths of 153 (Figure 10a) and 106 (Figure 10b) nm for the PAPBZ films having thicknesses of 10 and 26.4 μm, respectively, and of 26.6 (Figure 10c) and 29.0 (Figure 10d) nm for the BAPBZ films having thicknesses of 12.9 and 22.1 μm, respectively, based on AFM images. As a result, the surfaces of the BAPBZ polymer films (Figure 10c,d) were smoother than those of the PAPBZ monomer films, indicating that the polymer chains enhanced the film stability. Furthermore, this phenomenon arose because the trans-to-cis isomerization became more difficult for the high-molecular-weight BAPBZ polymer and, thereby, required more energy to reach completion. In addition, the long-range order of the alternative lamellar morphology was evident, with the cis form of the azobenzene units providing the dark lines of the valleys of the waves and the trans form of the azobenzene units providing the bright lines of the crests of the waves. We calculated the theoretical grating spatial period length based on the typical Bragg equation: $2d \sin \theta = n\lambda$; the theoretical d-spacing period length was 1.91 μm (calculated from $\theta = 8°$ from the incident angle for the reference beam, $n = 1$, and $\lambda = 532$ nm from the polarized green light), consistent with the values determined from the AFM images (ca. 1.85 μm).

The diffraction efficiency increased upon increasing the recording time for all of the azobenzene-containing compounds and for their different thicknesses. The diffraction efficiency of the monomer PAPBZ (13.2−20.5) after recording for 180 min was higher than that for the polymer BAPBZ (0.2−0.26) after recording for 270 min, indicating that the high molecular weight of BAPBZ led to a lower rate of trans-to-cis isomerization because of restricted molecular motion, consistent with the results from Figure 9 based on UV

DOI: 10.1021/acsapm.9b01079
ACS Appl. Polym. Mater. 2020, 2, 791−804

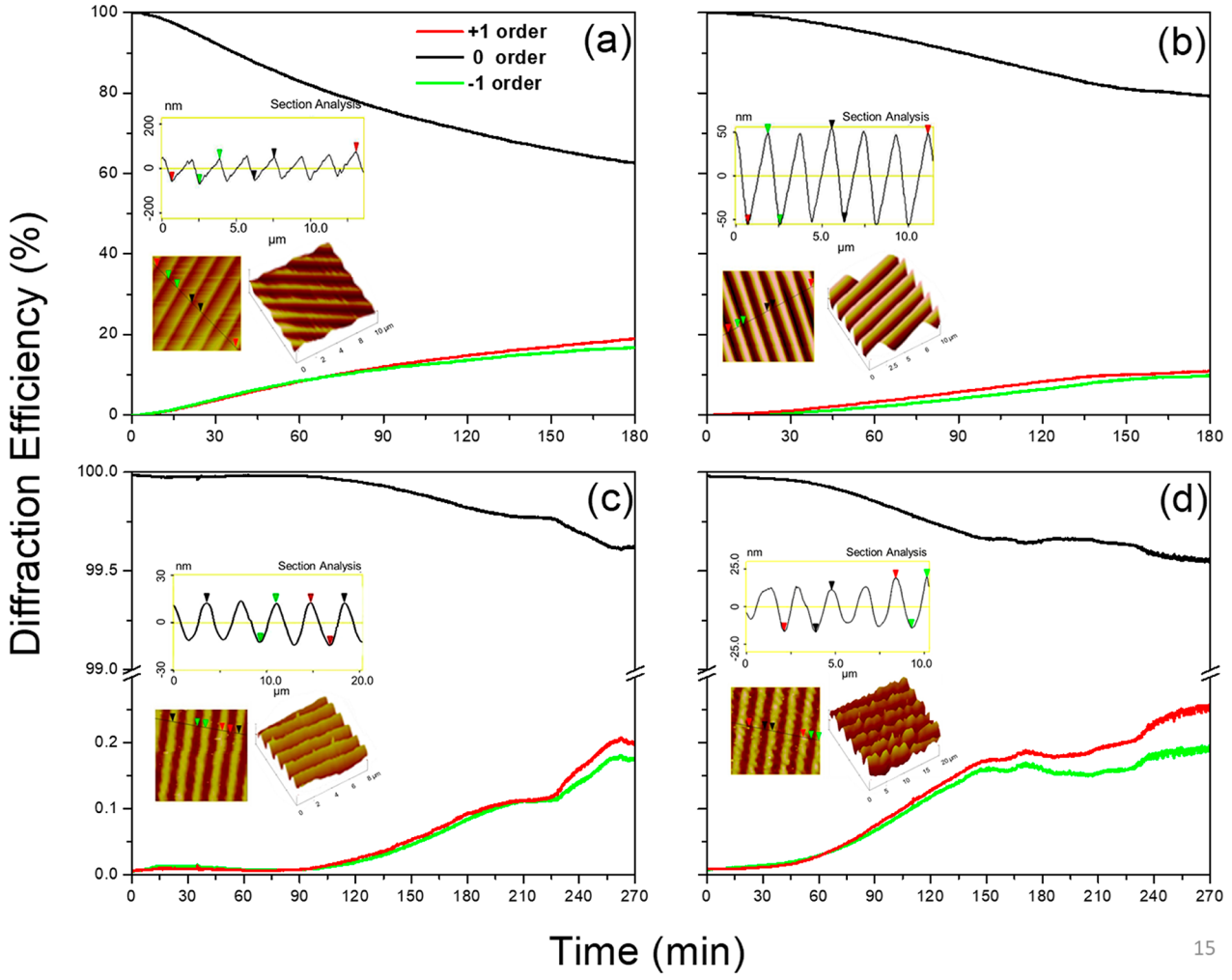

Figure 10. Diffraction efficiencies, height profiles, and 2D and 3D AFM images of films of (a,b) the monomer PAPBZ having thicknesses of (a) 10 and (b) 26.4 μm and of (c,d) the polymer BAPBZ having thicknesses of (c) 12.9 and (d) 22.1 μm, after exposure to laser light.

spectroscopic analysis. The diffraction efficiency for the monomer PAPBZ was greater than the values that we had obtained in previous studies by using noncovalent bonds to attach azobenzene groups to polymer side chains. The flexible alkyl side chains in this present case could enhance the surface modulation depth under the trans-to-cis isomerization and, thus, improve the diffraction efficiency.

CONCLUSIONS

We have prepared a new phenol-azo-pyridine benzoxazine monomer and a new bisphenol-azo-pyridine benzoxazine polymer through Mannich condensations of the precursor azo-pyridine-2NH_2, paraformaldehyde, and either phenol or bisphenol in toluene and EtOH. These materials are the first to incorporate azobenzene units into thermally stable pyridine-functionalized benzoxazines and into the main chains of polybenzoxazines. The phenol-azo-pyridine benzoxazine monomer underwent ROP through thermal curing at a temperature of 240 °C, providing a facile route to its polybenzoxazine, while the bisphenol-azo-pyridine benzoxazine polymer underwent cross-linking polymerization through thermal curing at a temperature of 300 °C, providing a high-density cross-linked polybenzoxazine. Because of the presence of the azobenzene units in these materials, we studied the photoresponsivities of the phenol-azo-pyridine benzoxazine monomer and bisphenol-azo-pyridine benzoxazine polymer. Under UV irradiation, the trans isomers of both the benzoxazine monomer and polymer were converted completely into their cis isomers after 30 min, and their cis isomers reverted back to their original trans isomers after storing in the dark for 24 h. The degrees of isomerization of the phenol-azo-pyridine benzoxazine monomer and the bisphenol-azo-pyridine benzoxazine polymer were 19.3 and 13.9%, respectively. Moreover, we fabricated SRGs from our synthesized benzoxazine monomer and polymer; they displayed long-range interface patterns, suggesting that these materials might have promising applications in optical devices.

ASSOCIATED CONTENT

Supporting Information

The Supporting Information is available free of charge at https://pubs.acs.org/doi/10.1021/acsapm.9b01079.

Experimental procedures and FTIR analyses of azo-hexyl-Br, pyridine-OH-2NO_2, azo-pyridine-2NO_2, azo-pyridine-2NH_2, monomer PAPBZ, and the polymer BAPBZ (PDF)

DOI: 10.1021/acsapm.9b01079
ACS Appl. Polym. Mater. 2020, 2, 791−804

AUTHOR INFORMATION

Corresponding Authors

*E-mail: tao.chen@nimte.ac.cn (T.C.).
*E-mail: kuosw@faculty.nsysu.edu.tw (S.W.K.).

ORCID

Tao Chen: 0000-0001-9704-9545
Shiao-Wei Kuo: 0000-0002-4306-7171

Notes

The authors declare no competing financial interest.

ACKNOWLEDGMENTS

This study was supported financially by the Ministry of Science and Technology, Taiwan, under Contracts MOST 106-2221-E-110-067-MY3, 108-2638-E-002-003-MY2, MOST 108-2218-E-110-013-MY3, and 108-2221-E-110-014-MY3. This work also supported by the National Natural Science Foundation of China (51773214).

REFERENCES

(1) Hartley, G. S. The cis-form of azobenzene. *Nature* **1937**, *140*, 281.
(2) Beharry, A. A.; Woolley, G. A. Azobenzene photoswitches for biomolecules. *Chem. Soc. Rev.* **2011**, *40*, 4422−4437.
(3) Mohamed, G. M.; Tu, J. H.; Huang, S. H.; Chiang, Y. W.; Kuo, S. W. Hydrogen bonding interactions affect the hierarchical self-assembly and secondary structures of comb-like polypeptide supramolecular complexes displaying photoresponsive behavior. *RSC Adv.* **2016**, *6*, 51456−51569.
(4) Bléger, D.; Hecht, S. Visible-light-activated molecular switches. *Angew. Chem., Int. Ed.* **2015**, *54*, 11338−11349.
(5) Sin, S. L.; Gan, L. H.; Hu, X.; Tam, K. C.; Gan, Y. Y. Photochemical and thermal isomerizations of azobenzene-containing amphiphilic diblock copolymers in aqueous micellar aggregates and in film. *Macromolecules* **2005**, *38*, 3943−3948.
(6) Blasco, E.; Piñol, M.; Oriol, L. Responsive linear-dendritic block copolymers. *Macromol. Rapid Commun.* **2014**, *35*, 1090−1115.
(7) Zheng, X. Y.; Wang, D.; Shuai, Z. G.; Zhang, X. Molecular dynamics simulations of the supramolecular assembly between an azobenzene-containing surfactant and α-cyclodextrin: role of photoisomerization. *J. Phys. Chem. B* **2012**, *116*, 823−832.
(8) Patra, D.; Zhang, H.; Sengupta, S.; Sen, A. Dual stimuli-responsive, rechargeable micropumps via "host-guest" interactions. *ACS Nano* **2013**, *7*, 7674−7679.
(9) Peng, C.; Zhao, W. K.; Wu, A. J.; Zhou, N.; Chen, S. Self-assembly between photoresponsive azobenzene-based dications and thermally sensitive PNIPAM-b-PAA block copolymers in aqueous solution. *J. Polym. Res.* **2018**, *25*, 63.
(10) Hvilsted, S.; Sánchez, C.; Alcala, R. The volume holographic optical storage potential in azobenzene containing polymers. *J. Mater. Chem.* **2009**, *19*, 6641−6648.
(11) Bruder, F. K.; Hagen, R.; Roelle, T.; Weiser, M. S.; Faecke, T. From the surface to volume: concepts for the next generation of optical-holographic data-storage materials. *Angew. Chem., Int. Ed.* **2011**, *50*, 4552.
(12) Lv, J.-a.; Liu, Y.; Wei, J.; Chen, E.; Qin, L.; Yu, Y. Photocontrol of fluid slugs in liquid crystal polymer microactuators. *Nature* **2016**, *537*, 179−184.
(13) Lu, X.; Guo, S.; Tong, X.; Xia, H.; Zhao, Y. Tunable photocontrolled motions using stored strain energy in malleable azobenzene liquid crystalline polymer Actuators. *Adv. Mater.* **2017**, *29*, 1606467.
(14) Zhang, W.; Yoshida, K.; Fujiki, M.; Zhu, X. Unpolarized-light-driven amplified chiroptical modulation between chiral aggregation and achiral disaggregation of an azobenzene-alt-fluorene copolymer in limonene. *Macromolecules* **2011**, *44*, 5105−5111.
(15) Wang, L.; Yin, L.; Zhang, W.; Zhu, X.; Fujiki, M. Circularly polarized light with sense and wavelengths to regulate azobenzene supramolecular chirality in optofluidic medium. *J. Am. Chem. Soc.* **2017**, *139*, 13218−13226.
(16) Mohamed, M. G.; Hsiao, C.-H.; Hsu, K.-C.; Lu, F.-H.; Shih, H.-K.; Kuo, S.-W. Supramolecular functionalized polybenzoxazines from azobenzene carboxylic acid/azobenzene pyridine complexes: synthesis, surface properties, and specific interactions. *RSC Adv.* **2015**, *5*, 12763−12772.
(17) Cheng, Z.; Ma, S.; Zhang, Y.; Huang, S.; Chen, Y.; Yu, H. Photomechanical motion of liquid-crystalline fibers bending away from a light source. *Macromolecules* **2017**, *50*, 8317−8324.
(18) Mohamed, M. G.; Hsiao, C. H.; Luo, F.; Dai, L.; Kuo, S. W. Multifunctional polybenzoxazine nanocomposites containing photoresponsive azobenzene units, catalytic carboxylic acid groups, and pyrene units capable of dispersing carbon nanotubes. *RSC Adv.* **2015**, *5*, 45201−45212.
(19) Oliveira, O. N., Jr.; dos Santos, D. S.; Balogh, D. T.; Zucolotto, V.; Mendonca, C. R. Optical storage and surface-relief gratings in azobenzene-containing nanostructured film. *Adv. Colloid Interface Sci.* **2005**, *116*, 179−192.
(20) Priimagi, A.; Vapaavuori, J.; Rodriguez, F. J.; Faul, C. F. J.; Heino, M. T.; Ikkala, O.; Kauranen, M.; Kaivola, M. Hydrogen-bonded polymer-azobenzene complexes: enhanced photoinduced birefringence with high temporal stability through interplay of intermolecular interactions. *Chem. Mater.* **2008**, *20*, 6358−6363.
(21) Kravchenko, A.; Shevchenko, A.; Ovchinnikov, V.; Priimagi, A.; Kaivola, M. Optical Interference Lithography Using Azobenzene-Functionalized Polymers for Micro- and Nanopatterning of Silicon. *Adv. Mater.* **2011**, *23*, 4174−4177.
(22) Vapaavuori, J.; Bazuin, C. G.; Priimagi, A. Supramolecular design principles for efficient photoresponsive polymer-azobenzene complexes. *J. Mater. Chem. C* **2018**, *6*, 2168−2188.
(23) Koskela, J. E.; Vapaavuori, J.; Hautala, J.; Priimagi, A.; Faul, C. F. J.; Kaivola, M.; Ras, R. H. A. Surface-relief gratings and stable birefringence inscribed using light of broad spectral range in supramolecular polymer-bisazobenzene complexes. *J. Phys. Chem. C* **2012**, *116*, 2363−2370.
(24) Liu, M.; Yin, L.; Wang, L.; Miao, T.; Cheng, X.; Wang, Y.; Zhang, W.; Zhu, X. Synthesis of monodisperse aromatic azo oligomers toward gaining new insight into the isomerization of π-conjugated azo systems. *Polym. Chem.* **2019**, *10*, 1806−1811.
(25) Wang, K.; Yin, L.; Miu, T.; Liu, M.; Zhao, Y.; Chen, Y.; Zhou, N.; Zhang, W.; Zhu, X. Design and synthesis of a novel azobenzene-containing polymer both in the main- and side-chain toward unique photocontrolled isomerization properties. *Mater. Chem. Front.* **2018**, *2*, 1112−1118.
(26) Yin, L.; Liu, M.; Zhao, Y.; Zhang, S.; Zhang, W.; Zhang, Z.; Zhu, X. Supramolecular chirality induced by chiral solvation in achiral cyclic Azo-containing polymers: topological effects on chiral aggregation. *Polym. Chem.* **2018**, *9*, 769−776.
(27) Wang, L.; Pan, X.; Zhao, Y.; Chen, Y.; Zhang, W.; Tu, Y.; Zhang, Z.; Zhu, J.; Zhou, N.; Zhu, X. A straightforward protocol for the highly efficient preparation of main-chain azo polymers directly from bisnitroaromatic compounds by the photocatalytic process. *Macromolecules* **2015**, *48*, 1289−1295.
(28) Natansohn, A.; Rochon, P. Photoinduced motions in azo-containing polymers. *Chem. Rev.* **2002**, *102*, 4139−4176.
(29) Huang, C. W.; Ji, W. Y.; Kuo, S. W. Stimuli-responsive supramolecular conjugated polymer with phototunable surface relief grating. *Polym. Chem.* **2018**, *9*, 2813−2820.
(30) Huang, C. W.; Wu, P. W.; Su, W. H.; Zhu, C. Y.; Kuo, S. W. Stimuli-responsive supramolecular materials: photo-tunable properties and molecular recognition behavior. *Polym. Chem.* **2016**, *7*, 795−806.
(31) Ni, Y.; Li, X.; Hu, J.; Huang, S.; Yu, H. Supramolecular liquid-crystalline polymer organogel: fabrication, multiresponsiveness, and holographic switching properties. *Chem. Mater.* **2019**, *31*, 3388−3394.

DOI: 10.1021/acsapm.9b01079
ACS Appl. Polym. Mater. 2020, 2, 791−804

(32) Burke, W. J. 3,4-Dihydro-1,3,2H-benzoxazines. reaction of *p*-substituted phenols with N, N-dimethylolamines. *J. Am. Chem. Soc.* **1949**, *71*, 609−612.
(33) Ning, X.; Ishida, H. Phenolic materials via ring-opening polymerization: Synthesis and characterization of bisphenol-A based benzoxazines and their polymers. *J. Polym. Sci., Part A: Polym. Chem.* **1994**, *32*, 1121−1129.
(34) Ishida, H. *Book of Benzoxazine Resins*; Ishida, H., Aaga, T., Eds.; Elsevier: Amsterdam, The Netherlands, 2011; pp 3−81.
(35) Hu, W. H.; Huang, K. W.; Kuo, S. W. Heteronucleobase-functionalized benzoxazine: synthesis, thermal properties, and self-assembled structure formed through multiple hydrogen bonding interactions. *Polym. Chem.* **2012**, *3*, 1546−1554.
(36) Lin, C. H.; Shih, Y. S.; Wang, M. W.; Tseng, C. T.; Juang, T. Y.; Wang, C. F. Emission and surface properties of main-chain type polybenzoxazine with pyridinyl moieties. *RSC Adv.* **2014**, *4*, 8692−8698.
(37) Mohamed, M.; Kuo, S. W. Polybenzoxazine/polyhedral oligomeric silsesquioxane (POSS) nanocomposites. *Polymers* **2016**, *8*, 225.
(38) El-Mahdy, A. F. M.; Kuo, S. W. Direct synthesis of poly(benzoxazine imide) from an ortho-benzoxazine: its thermal conversion to highly cross-linked polybenzoxazole and blending with poly(4-vinylphenol). *Polym. Chem.* **2018**, *9*, 1815−1826.
(39) Chernykh, A.; Liu, J. P.; Ishida, H. Synthesis and properties of a new crosslinkable polymer containing benzoxazine moiety in the main chain. *Polymer* **2006**, *47*, 7664−7669.
(40) Tsai, C. C.; Gan, Z.; Kuo, S. W. Using benzoxazine chemistry and bio-based triblock copolymer to prepare functional porous polypeptide capable of efficient dye adsorption. *Polym. Chem.* **2018**, *9*, 3684−3693.
(41) Ye, Y. S.; Huang, Y. J.; Chang, F. C.; Xue, Z. G.; Xie, X. L. Synthesis and characterization of thermally cured polytriazole polymers incorporating main or side chain benzoxazine crosslinking moieties. *Polym. Chem.* **2014**, *5*, 2863−2871.
(42) Hanbeyoglu, B.; Kiskan, B.; Yagci, Y. Hydroxyl functional polybenzoxazine precursor as a versatile platform for post-polymer modifications. *Macromolecules* **2013**, *46*, 8434−8440.
(43) Zhang, K.; Yu, X.; Kuo, S. W. Main-chain-type poly(benzoxazine-co-imide-co-siloxane) based cross-linked network exhibiting outstanding dielectric and thermal properties. *Polym. Chem.* **2019**, *10*, 2387−2396.
(44) Abuzeid, H. R.; El-Mahdy, A. F. M.; Ahmed, M. M. M.; Kuo, S. W. Triazine-functionalized covalent benzoxazine framework for direct synthesis of N-doped microporous carbon. *Polym. Chem.* **2019**, *10*, 6010−6020.
(45) Lin, R. C.; Kuo, S. W. Well-defined benzoxazine/triphenylamine-based hyperbranched polymers with controlled degree of branching. *RSC Adv.* **2018**, *8*, 13592−13611.
(46) Wang, Y. X.; Ishida, H. Cationic ring-opening polymerization of benzoxazines. *Polymer* **1999**, *40*, 4563−4570.
(47) Sudo, A.; Kudoh, R.; Nakayama, H.; Arima, K.; Endo, T. Selective formation of poly(N, O-acetal) by polymerization of 1,3-benzoxazine and its main chain rearrangement. *Macromolecules* **2008**, *41*, 9030−9034.
(48) Wang, C. F.; Su, Y. C.; Kuo, S. W.; Huang, C. F.; Sheen, Y. C.; Chang, F. C. Low-surface-free-energy materials based on polybenzoxazines. *Angew. Chem., Int. Ed.* **2006**, *45*, 2248−2251.
(49) Zhang, K.; Tan, X.; Wang, Y.; Ishida, H. Unique self-catalyzed cationic ring-opening polymerization of a high performance deoxybenzoin-based 1;3-benzoxazine monomer. *Polymer* **2019**, *168*, 8−15.
(50) Kuo, S. W.; Wu, Y. C.; Wang, C. F.; Jeong, K. U. Preparing low-surface-energy polymer materials by minimizing intermolecular hydrogen-bonding interactions. *J. Phys. Chem. C* **2009**, *113*, 20666−20673.
(51) Arslan, M.; Motallebzadeh, A.; Kiskan, B.; Demirel, A. L.; Kumbaraci, I. V.; Yagci, Y. Combining benzoxazine; ketene chemistries for self-healing of high performance thermoset surfaces. *Polym. Chem.* **2018**, *9*, 2031−2039.
(52) Zhang, K.; Ishida, H. Thermally stable polybenzoxazines via ortho-norbornene functional benzoxazine monomers: unique advantages in monomer synthesis, processing and polymer properties. *Polymer* **2015**, *66*, 240−248.
(53) Zhang, K.; Yu, X. Catalyst-free and low-temperature terpolymerization in a single component benzoxazine resin containing both norbornene and acetylene functionalities. *Macromolecules* **2018**, *51*, 6524−6533.
(54) Wu, J.; Xi, Y.; Mccandless, G. T.; Xie, Y.; Menon, R.; Patel, Y.; Yang, D. J.; Iacono, S. T.; Novak, B. M. Synthesis and characterization of partially fluorinated polybenzoxazine resins utilizing octafluorocyclopentene as a versatile building block. *Macromolecules* **2015**, *48*, 6087−6095.
(55) Zhang, K.; Han, L.; Froimowicz, P.; Ishida, H. A smart latent catalyst containing otrifluoroacetamide functional benzoxazine: precursor for low temperature formation of very high Performance polybenzoxazole with low dielectric constant and high thermal stability. *Macromolecules* **2017**, *50*, 6552−6560.
(56) Zhang, K.; Shang, Z.; Evans, C. J.; Han, L.; Ishida, H.; Yang, S. Benzoxazine atropisomers: Intrinsic atropisomerization mechanism and conversion to high performance thermosets. *Macromolecules* **2018**, *51*, 7574−7585.
(57) Tamami, B.; Yeganeh, H. Synthesis and characterization of novel aromatic polyamides derived from 4-aryl-2,6-bis(4-aminophenyl) pyridines. *Polymer* **2001**, *42*, 415−420.
(58) Tamami, B.; Yeganeh, H. Preparation and properties of novel polyimides derived from 4-aryl-2,6 bis(4-amino phenyl)pyridine. *J. Polym. Sci., Part A: Polym. Chem.* **2001**, *39*, 3826−3831.
(59) Liaw, D.-J.; Wang, K.-L.; Chang, F.-C.; Lee, K.-R.; Lai, J.-Y. Novel poly(pyridine imide) with pendent naphthalene groups: Synthesis and thermal, optical, electrochemical, electrochromic, and protonation characterization. *J. Polym. Sci., Part A: Polym. Chem.* **2007**, *45*, 2367−2374.
(60) Liaw, D.-J.; Wang, K.-L.; Chang, F.-C. Novel organosoluble poly(pyridine-imide) with pendent pyrene group: synthesis, thermal, optical, electrochemical, electrochromic, and protonation characterization. *Macromolecules* **2007**, *40*, 3568−3574.
(61) Frank, R. L.; Seven, R. P. Pyridines. IV. A study of the chichibabin synthesis. *J. Am. Chem. Soc.* **1949**, *71*, 2629−2635.
(62) Katritzky, A.; Rees, C. *Comprehensive Heterocyclic Chemistry*; Oxford: Pergamon, 1984; Vol. *2*; p 395.
(63) Weiss, M. Acetic acid—ammonium acetate reactions. an improved Chichibabin pyridine synthesis. *J. Am. Chem. Soc.* **1952**, *74*, 200−202.
(64) Wang, X.; Li, Y.; Gong, C.; Zhang, S.; Ma, T. Synthesis and characterization of novel soluble pyridine-containing polyimides based on 4-phenyl-2,6-bis[4-(4-aminophenoxy)phenyl]-pyridine and various aromatic dianhydrides. *J. Appl. Polym. Sci.* **2007**, *104*, 212−219.
(65) Lin, C. H.; Shih, Y. S.; Wang, M. W.; Tseng, C. Y.; Chen, T. C.; Chang, H. C.; Juang, T. Y. Pyridinyl-containing benzoxazine: Unusual curing behaviors with epoxy resins. *Polymer* **2014**, *55*, 1666−1673.
(66) Shibayama, Y.; Kawauchi, T.; Takeichi, T. Synthesis and properties of polybenzoxazines containing pyridyl group. *High Perform. Polym.* **2014**, *26*, 60−68.
(67) Kumar, G. S.; Neckers, D. C. Photochemistry of azobenzene-containing polymers. *Chem. Rev.* **1989**, *89*, 1915−1925.
(68) Xie, Z.; He, H. F.; Deng, Y. H.; Wang, X. G.; Liu, C. Y. Three-arm star compounds composed of 1,3,5-tri(azobenzeneethynyl)-benzene cores and flexible PEO arms: synthesis, optical functions, hybrid Ormosil gel glasses. *J. Mater. Chem. C* **2013**, *1*, 1791.

DOI: 10.1021/acsapm.9b01079
ACS Appl. Polym. Mater. 2020, 2, 791−804